DESIGN AND TESTING OF A SOWING DRONE BASED ON RICE PRECISION STRIP SEEDING
/
水稻精量化条直播播种无人机的设计与试验

Liangchen HOU[1)], Xin HAN[*1)], Yubin LAN[*1)], Jingbo BAI[2)], Zhikang DING[1)], Xuejian ZHANG[3)], Maochang SONG[1)], Kailu WANG[1)]

[1)]School of Agricultural and Food Science, Shandong University of Technology, Zibo (255000), China;
[2)]Shandong Siyuan Agricultural development Co., LTD, Zibo (25000), China;
[3)]Institute of Agricultural Economics and Information Technology, Ningxia Academy of Agricultural and Forestry Sciences, Ningxia (750002), China
Tel: +86-15953359191; +86-13922707507; E-mail: hanxin_1979@163.com ylan@sdut.edu.cn
DOI: https://doi.org/10.35633/inmateh-73-29

Keywords: *UAV, direct sowing in strips, external grooved wheel seeder, simulation analysis, control system*

ABSTRACT
In order to solve the problem that the wind field disturbs the trajectory of falling seeds and causes the seeds to be unable to be arranged in equidistant rows when the UAV is spreading rice, a shot seeding device that can sow five rows of pelleted rice seeds at the same time was designed. The unit is centered on an external grooved wheel seed metering device and a seed acceleration unit for row seeding and hole sowing. The airflow simulation of the rotor wind field of the UAV was carried out by simulation software to explore the changes in the wind field of the UAV during operation. The position where the wind field disturbance is minimized is chosen for the seed guide tube arrangement. The position with the least wind field disturbance is chosen to arrange the seed guide tube and combine it with a seed acceleration device to reduce the influence of the UAV wind field airflow on the direction of seed movement. The operational effectiveness of the seeding device with and without wind was verified by an indoor test and an outdoor flight seeding test, respectively. Simulation results show that: when the mouth of the seed guide pipe is 0.9 m away from the paddle, the wind field has the smallest influence on the sowing results. The results of the bench test show that: when the rotational speed is 30-45 r/min, the coefficient of variation of the discharge rate of each row (CVR) and total seed discharge rate stability (CVT) are less than 1.98% and 0.84%, and the seed breakage rate is less than 0.95%, which all conform to the UAV fly sowing industry standards. The outdoor mud box test shows that: when the baffle angle changes by 26%, 58%, and 71%, each slot wheel hole can store 5-10, 3-5 and 1-3 seeds respectively, and the UAV operates at a speed of 2 m/s-3 m/s, the pass rate of hybrid rice is greater than 86%, which meets the agronomic requirements of rice sowing operation.

摘要
为解决无人机在水稻撒播时，普遍存在风场扰动种子下落的轨迹和种子无法成穴排布的问题，设计了一种可同时播种六行颗粒状水稻种子的射种装置。该装置由一个外槽轮式排种装置和种子加速装置为核心，实现了精准行播和穴播的功能。通过仿真软件对无人机进行了旋翼风场的气流仿真模拟，探究风场的变化特性。确定风场扰动最小的位置去布置导种管。加速装置和无人机的气流分析都是为了减少无人机风力对种子运动方向的影响。在室内试验和室外飞行播种试验中，分别验证在无风场和有风场下播种装置的作业效果。仿真结果表明：导种管道口距离桨叶为 0.9m 时，风场对播种结果影响最小；台架试验结果表明：转速处于 30-45r/min 时，每行排种率的变异系数小于 1.98%、总排量稳定性的变异系数小于 0.84%、种子破损率小于 0.95%等都符合无人机飞播行业标准；室外泥盒试验表明：挡板角度变化 26%、58%、71%时，每个槽轮孔可以分别储存 5-10 粒、3-5 粒、1-3 粒种子，且无人机以 2m/s-3m/s 速度下作业，杂交稻合格率均大于 86%，满足水稻直播作业的农艺要求.

INTRODUCTION
As one of the three major food crops in the world, rice is closely related to people's lives. Ensuring rice yield is of great significance to meet the food demand of China and the world. Rice mechanized planting operation is the most critical and weakest link in the three major production processes of rice cultivation, planting, and harvesting. Moreover, rice planting is the most important factor hindering the production of mechanized rice at present. Therefore, it is very necessary to improve the efficiency of rice mechanized planting and the level of automatic operation (*Luo et al., 2019*).

In recent years, agricultural aviation technology has been developing rapidly at home and abroad because of its advantages of not being restricted by the operating environment, higher operating efficiency, less impact on crop growth, and low operating costs at the same time. Agricultural aviation assumes an important role in the development of modern precision aerial agriculture. In this study, the autonomous design of UAV can achieve route planning, land-like flight, autonomous obstacle circling, automatic return, flexible take-off, and landing through the data fusion of multiple sensors. It also proves that the efficiency, cost, and stability of land-based equipment are not as good as UAVs. Super-hybrid rice is a type of hybrid rice with greater tillering capacity and higher yields. When sowing by direct seeding technology, only 1~3 grains/hole are generally needed, of which 2 grains/hole are preferred, with a plant spacing of about 10 cm and a row spacing of about 30 cm. but often land equipment operates at a slower speed. Therefore, there is an urgent need to study the precision sowing technology of hybrid rice using drones as a carrier (*Zhou et al., 2014*). In this paper, hybrid rice is taken as the research object, and the research and design are carried out for precise and quantitative row sowing and hole sowing (*Luo et al., 2019*).

At present, drone seeding is categorized as row seeding and spread seeding, but regular distribution of cavities cannot be achieved. The field of seeding using drones has developed rapidly in recent years. In response, the land-based equipment has the disadvantages of easily getting stuck in the soil and low operating efficiency. Seeding by drones has become a new type of rice cultivation (*Wan et al., 2021*). Among them, Gao Xuemei et al. developed a rice and fertilizer spreading device. The device mainly used centrifugal force to spill rice seeds along the outlet of the spreading device. However, the influence of the wind field of the UAV and the parameter matching problem of the spreading disc resulted in poor spreading uniformity (*Gao et al., 2022*).

Huang Xiaomao et al. designed a row sowing device for both rice and oilseed rape. The device adopted a split seed dispenser and folded seed guide tube program, which could reduce the wind field impact and achieved the position of the falling seeds arranged in strips. However, the speed of rice seed drop plus was limited, resulting in the seeds not being able to penetrate 1-2 cm below the soil, making it difficult to meet agronomic requirements. Rice seeds floated on the soil surface and were easily eaten by birds and rats. The seeds also floated away due to the external wind (*Huang et al., 2020; Huang et al., 2022*); Li Wencheng et al. designed an oilseed rape drone fly sowing device, which could realize oilseed rape in rows and rows. However, the seed guide tube he designed was too long, which was a big hidden danger to the safety of the flight (*Li et al., 2020; Zhang et al., 2020*); Song Cancan et al. designed a method to achieve spreading through high-speed airflow, which in turn achieved uniform fertilizer spreading. However, the uniformity of that program was general (*Song et al., 2018; Song et al., 2020*).

He Weizhuo et al. designed a seed acceleration device with friction wheel force, which accelerated the rice seed significantly and did not hurt the seed. This solution could achieve row sowing but not hole sowing, improve the uniformity of the position of seed fall and reduce the effect of airflow from the drone on the trajectory of the seed. In this study, the seed sowing method was improved by increasing friction based on others（*He et al., 2022*). At the same time, an external grooved wheel seed metering device was designed to achieve an equalized distance between two adjacent seed-filled holes. The wind field airflow was simulated under the UAV by simulation software to simulate the change of wind field under the rotor surface, so that the optimal location of the seed discharge point could be determined and the effect of UAV wind on the seed trajectory could be reduced (*Shen et al., 2018; Zhang et al., 2019*).

In this paper, an external grooved wheel seed metering device is designed, where the volume of the grooves and the rotational speed of the grooved wheel can be precisely controlled and adjusted to accurately group the seeds and adjust the seed flow rate and the falling frequency (*Zeng et al., 2021*). The acceleration of the seed by the friction wheel reduces the effect of the wind field on the seed trajectory and allows the seed to penetrate deeper into the soil. Compared with other drone seeding methods, this solution can make the seed drop location evenly distributed and reduce the impact of the wind field on the seed trajectory. It provides a reference for the subsequent UAV rice direct seeding technology.

MATERIALS AND METHODS

Flying seeding drone machine structure and principle

The whole machine is divided into three main parts: drone platform, seed discharge device, and seeding device, as shown in Fig. (1). Among them, the grooved wheel seed discharger and seed acceleration device are fixedly connected to the frame of the UAV through fixing parts.

Fig. 1 - Three-dimensional roadmap

Fig. 2 - Physical drawing of rice flying seeding drone

This experiment uses an independently designed X8 co-axial counter-propeller UAV as a power platform to ensure hovering and flight attitude during operation. The seeding device is divided into three processes: seed filling, seed carrying, and seed shooting. The seed-filling process is the free fall of rice seeds from the seed box to the inlet of the grooved wheel under the effect of gravity. The seed is transported to the accelerating device during the rotation of the grooved wheel. The trough wheel is rotated by a 42-step motor, and the rotational speed is controlled by a handheld remote control that establishes communication with the motor drive module and the signal transmitter. Different rotational speeds control the flow of seed output from the trough wheel per unit of time. The chute wheels uniformly control the seed drop, and then the seed dispenser carries the seed from each chute wheel opening to the acceleration device. The acceleration device consists of two motors that control the opposite rotation of two friction wheels. The acceleration unit consists of two motors that control the opposite rotation of two friction wheels. The friction wheels provide the seeds with a friction force, and then the seeds enter the acceleration device and are instantly squeezed by the two friction wheels to use the friction force to accelerate them, and then after passing through the pipeline, they pass through the wind field under the rotor blades of the UAV and are shot into the soil at a distance of 1-2 cm, to complete the fly sowing operation.

Table 1

Rice seeding drone-specific parameters

Parametric	Numerical value
Overall dimensions (L×W×H)/(mm)	1100 ×1100×950（Arm deployment） 600 ×600×950（Arm Removal）
Seeding method	Strip sowing, hole sowing
Number of lines of work	6
Sowing rate (dry weight of rice seed)/ (kg/min)	1-3
The rotational speed of groove wheel / (r/min)	30-45
Working width / (m)	1-2.1
Operating altitude / (m)	1-2
Operational flight speed / (m/s)	1.5-2.5
Seedbox capacity / (kg)	18
Maximum Endurance / (min)	16
Overall quality / (kg)	35.06

Sowing device layout

Rice UAV flying and seeding control system

The whole control system is divided into the UAV flight control system, sowing control system, and monitoring system, as shown in Figure 3 below. The mission platform consists of two parts: the trough wheel and the acceleration device. The trough wheel is printed by a 3D printer using PLA material to print out the mold and installed for use. The grooved wheel controls the rotational speed and thus the flow of rice seeds through a type 42 stepper motor and a motor driver. The groove baffle of the groove wheel can be rotated along the axis at an appropriate angle to effectively control the size of the groove hole and the quantity of rice seeds.

The acceleration device uses a friction wheel driven by a motor to accelerate the rice seed and then complete the sowing operation. The friction wheel is made of rubber, which is elastic and does not harm the rice seeds. The maximum speed of the motor is up to 9000 r/min, which ensures a high seed ejection speed. The motor is controlled by an electronic speed controller (ESC). External stm32f1 microcontroller controls ESC and thus controls the friction wheel speed and stepping motor speed. One of the monitoring systems, consisting of a piezoresistive weight sensor. Sensor set two order alarm prompts, in the seed box balance of 5 kg and 2 kg when the remote control alarm occurs. The motors are set up to monitor the identification and alarm when one of the accelerators jams. In which the whole flight control system is linked to the seeding main controller for signal interaction and information transfer.

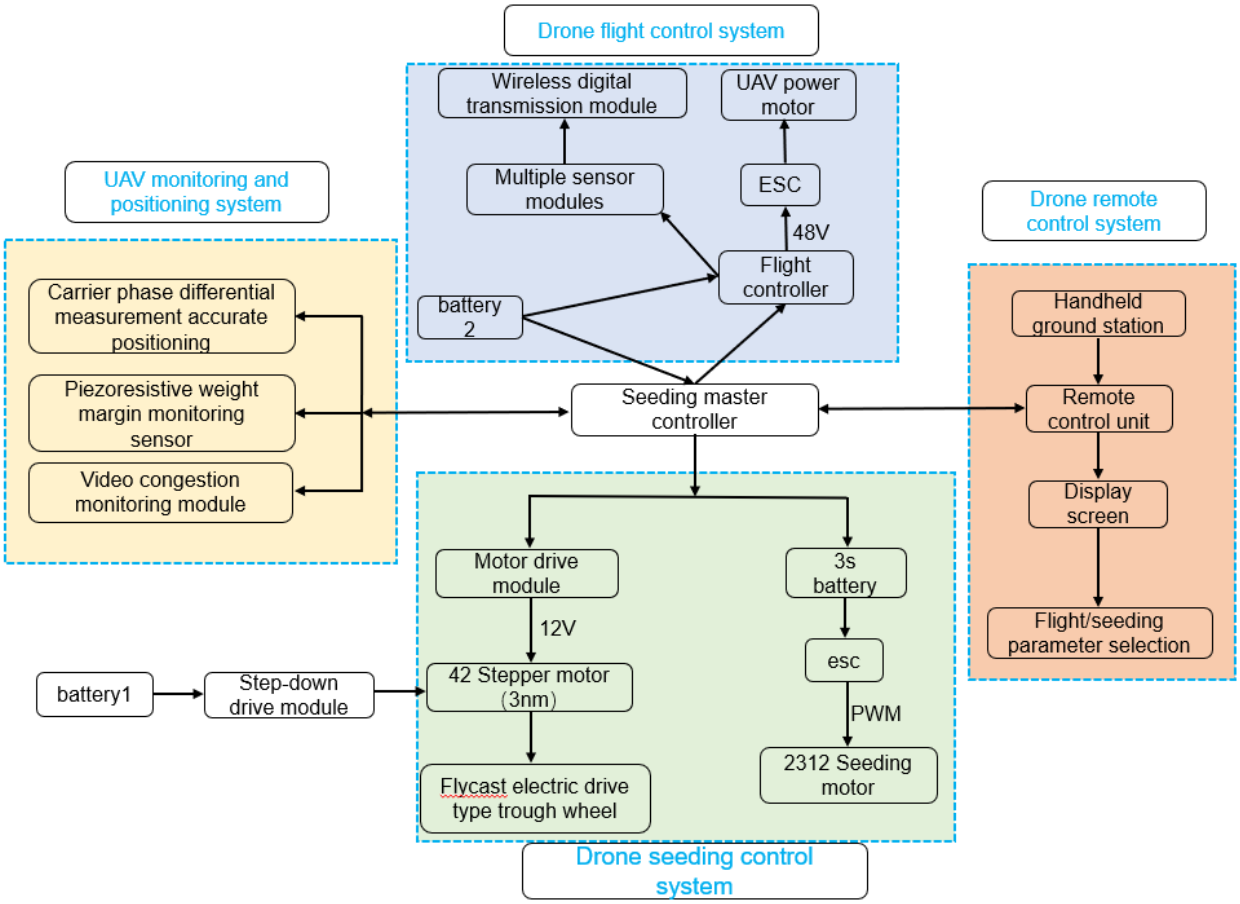

Fig. 3 - Block diagram of UAV rice seeding control system structure

The rice seeding UAV consists of the flight control system, ground control system, propulsion system, power system, and seeding control system as follows (4). The fuselage is made of carbon-brazed dimensional material, and the flight-sowing UAV control system adopts DJI-A3, including a control master module, power module, GPS module, LED module, Lightbridge2, and image transmission module *(Bian et al., 2024)*. The motors are DJI E5000 series, with a pull force of 7kg. Since the single-axis dual propellers have a 10%-30% power loss, the minimum single-axis pull force is 9.8kg. The arm carries sockets, which can be plugged and unplugged to reduce the storage volume. The flight control system is the brain of the UAV, mainly responsible for the autonomous flight of the UAV. The ground control system works in conjunction with the flight control system to control the flight of the UAV, and you can choose automatic flight settings or manual operation. The propulsion system is responsible for powering the UAV to climb, hover, fly, and land. The power system consists of a battery and a power distribution unit (PDU), which powers the propulsion system, the rice seeding system, and the flight control system. The rice seeding system consists of a seed supply system and a seed discharge system. The grooved wheel can precisely control the flow and frequency of the falling rice seeds, and the friction wheel is responsible for shooting the seeds under the soil in batches at intervals to achieve hole sowing.

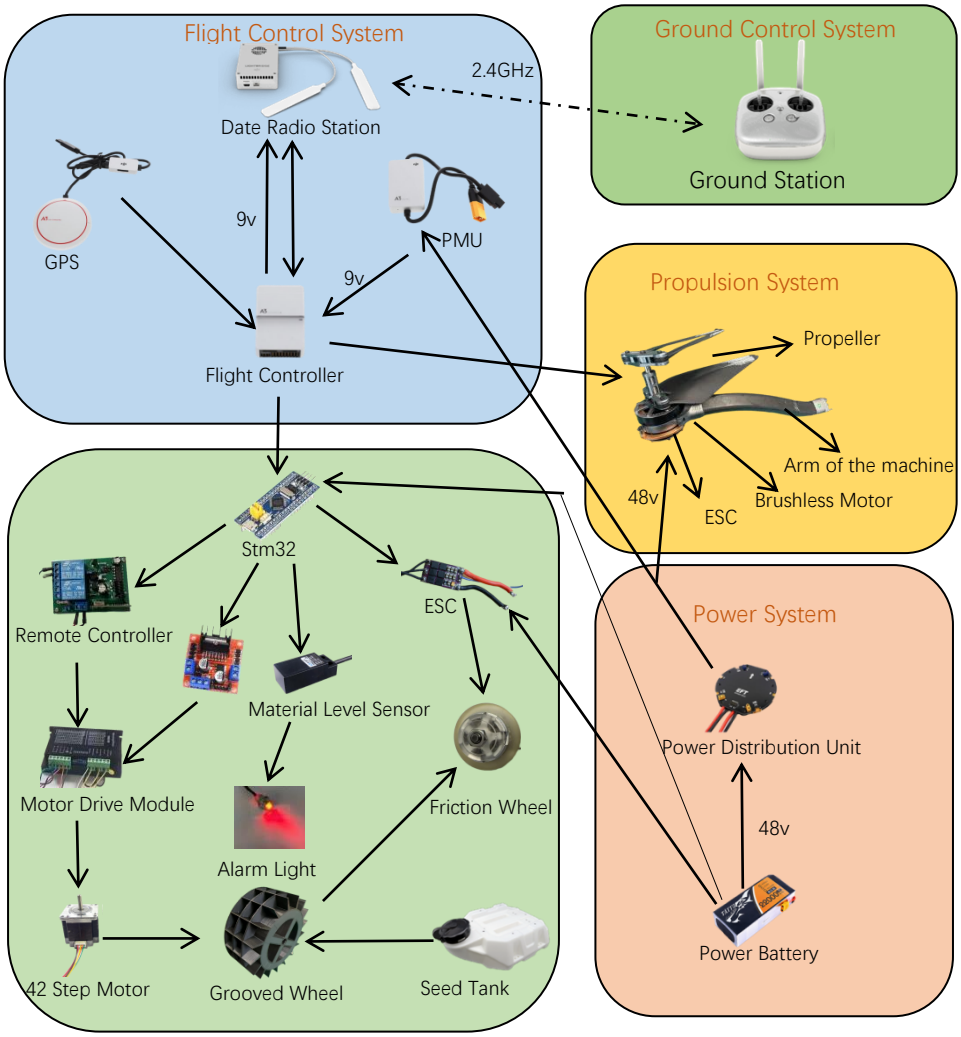

Fig. 4 - Components of the UAV and the workflow of each system

Design and parameterization of key seeding devices for rice drones

Seeder design

Rice seeds need to be treated before sowing. Firstly, the outer layer of the rice seed is wrapped with a layer of hard powder, which is rich in fertilizers and nutrients that promote the growth and development of the rice seed. The seeds are then hardened and treated to approximate the shape of a sphere. The hardness and volume can be customized in the device. This technique is called 'seed dressing'. In this paper, the rice seed is set as a sphere with a diameter of 5 mm.

The design of the friction wheel extrusion direct injection device is shown in Figure (5) below: the frequency of rice seed drop controlled by the grooved wheel of the previous link is 2 or 4 seeds in a group. The falling seeds then pass through the seed distributor into the gap between the two friction wheels. When the seed passes through the friction wheel A and friction wheel B, the two friction wheels rotate at a high speed in the opposite direction, giving the seed two friction forces in the same direction respectively, and quickly shoot the rice seed into the soil, the rice seed will have a short residence time in the guide and during the drop. In this paper, the motor is fixed inside the friction wheel, and the friction wheel is rotated by the motor. The accelerating motor is an external rotor brushless motor, and the model of the motor is DJI-2312A. In order to ensure that the seeds are in full contact with the friction wheels, the gap between the two friction wheels is set to 3.5 mm. The catheter is mounted at the bottom of the guide rail. Due to the error in the production process of the coated seeds, the diameters are slightly different. Setting a tension spring underneath the two motor holders allows the friction wheels to adapt to seeds of different diameters and reduces the seed breakage rate.

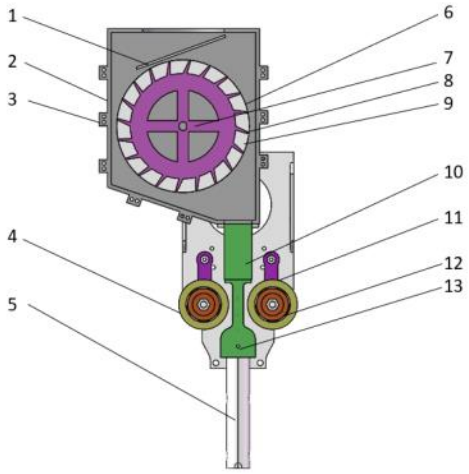

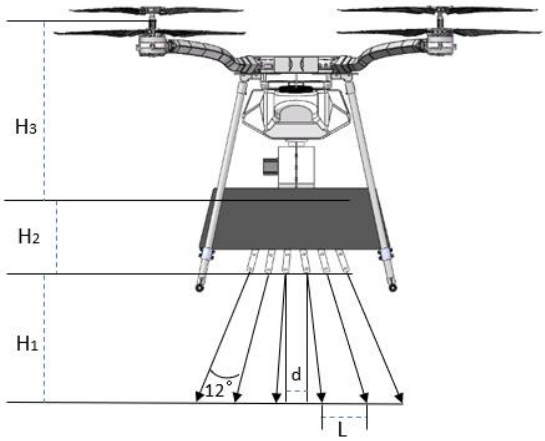

Fig. 5 - Overall structure of the sowing device **Fig. 6 - Key Component Arrangement**

1. Seed stopper; 2. Grooved wheel housing; 3. Screw fixing parts; 4. Rubber wheel; 5. Seed guide tube; 6. Adjusting stopper; 7. Rotating shaft; 8. Grooved wheel hole; 9. Grooved wheel; 10. Seed tube; 11. Flexible motor holder; 12. Brushless motor; 13. Guide rail

H1 refers to the direct distance between the pipe and the ground; H2 refers to the distance for seed acceleration; H3 is the distance between the rotor surface and the seed inlet, d refers to the distance between two neighboring pipes, and L refers to the row spacing

In this paper, coated rice seeds were used as the research object for sowing. Before the experiment, special equipment was used to wrap a layer of powder and solution containing nutrients such as fertilizer on the outer layer of the seeds. When the seeds were dried the outer layer of material hardened and the shape of the seeds was made into a ball shape. Compared to other drone seeding, such as centrifugal spreading (*Gao et al., 2022)* and seeding by gravity (*Huang et al., 2020*), it is not possible to give the seeds increased acceleration. In this paper, the device applies a strong friction force to the seed so that the seed has the initial speed to better cross the wind field and enter the soil. This can effectively realize the orderly arrangement of seeds on the ground and improve the uniformity of sowing. At the same time, the control to adjust the opening and closing angle between two neighboring seed dispensers can control the size of the row spacing, and the layout of the conduit and acceleration device is shown in Fig. 6.

At the same time, the hard texture of the coated seeds, rich in fertilizer and other nutrients will slowly dissolve in the water to promote seed germination, so that the layout reduces the risk of rice seeds floating on the surface of the soil being eaten by birds, rats, or even washed away by the rain, resulting in a lack of seedlings. At the same time, it also enables the seeds to be not affected by the ambient wind or the rotor winds of the drone resulting in an uneven density of the landing site, thus causing poor permeability in the later stages and thus triggering the risk of diseases and insect pests.

Grooved wheel design

In this paper, an external grooved wheel seed metering device is designed as shown in Fig. 7, where the number of seeds inside the groove is controlled by controlling the angle of baffle. Where the power of the groove wheel is provided by a stepper motor (3 Nm 42 stepper motor). The power is provided by the UAV battery (model 22000aAh, 6s, 25.2v). The power supply is connected to the buck module and a remote control system is established with the motor driver, signal receiver, and remote control. The remote control system of the grooved wheel is shown in Fig. 8 below, and the grooved wheel is equipped with six circles of grooved holes on the outside, with 20 grooved holes in each circle. The baffle plate is used to regulate the volume of the holes, the larger the opening of the baffle plate, the smaller the volume of the holes in the wheel and the smaller the inflow of rice seed. The groove wheel uses a 2.4 GHz remote control (AT9S PRO) with 12 buttons to control the start, stop and speed of the groove wheel. The microcontroller controls the speed of the seed metering motor, and its signal transmission is based on the 1, 2, 8, 9, and 10 buttons, so that the number of rice seeds falling into each groove is basically the same, reducing the missed seeding rate and repetition rate.

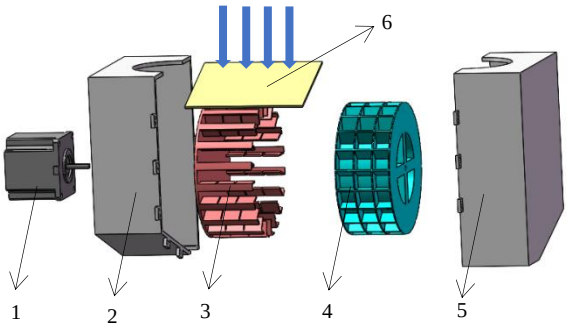

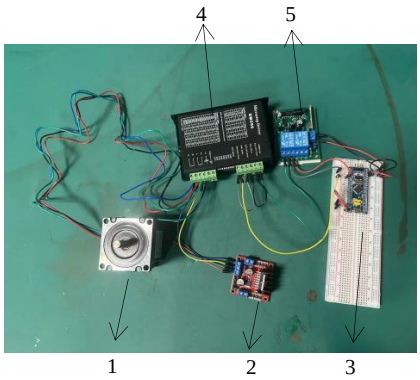

Fig. 7 - Seed Discharger Structure Diagram **Fig. 8 - Motor control system wiring diagram**

1 - 42 Stepping motor; 2 - Left grooved wheel housing; 3 - Seed stopper angle opening and closing plate; 4 - Grooved wheel; 5 – Right grooved wheel housing; 6 - Seed stopper; 1 - 42 Stepper motor; 2 - L298 motor drive module; 3 - Stm32 microcontroller; 4 - Motor driver; 5 – Receiver

The diameter of the grooved wheel, the structure and the number of holes have a greater impact on the performance of fly-sowing operations. When the sowing volume and operating speed are certain, the number of grooved wheel holes is inversely proportional to the rotational speed of the grooved wheel. If the diameter of the grooved wheel is too small, the grooved wheel rotational speed is high, which will lead to an increase in the rate of seed breakage; if the diameter of the grooved wheel is too large, the volume of the seed discharge device is large, which is not suitable for unmanned aerial sowing operations. Comprehensive consideration, the external dimensions of the grooved wheel are designed to be 95 mm in diameter and 101 mm in length. The grooved wheel has a number of slotted wheel holes on the outside to group the seeds.

In order to facilitate the smooth discharge of seeds from the groove, the wall of the groove side is designed to be an inclined quadrilateral with an inclination angle of 40°. Compared with a square, this structure not only makes it easier for seeds to escape from the groove, but also reduces the risk of the groove wheel getting stuck. The inclination of the groove wall is conducive to rapid seed filling and seeding. During operation, in order to ensure the seeding volume during fast flight operation, each groove is designed to be filled with 1-10 seeds, and the number of seeds can be freely adjusted.

The adjustment process is as follows: (1) baffle opening 0%, slot wheel hole in the maximum capacity of rice seed volume state, a single hole of about 10-15 grains, at this time the speed is higher, the seeding volume is larger, the flight speed is relatively fast suitable for strip seeding; (2) baffle opening 26%, slotted wheel hole can hold 5-10 rice seeds; (3) baffle opening 58%, slotted wheel hole can hold 3-5 rice seeds; (4) baffle opening 71%, and slotted wheel hole can hold 1-3 rice seeds.

Simulation environment construction

The airflow disturbance in the wind field of motion under the rotor of the UAV is large and has an effect on the trajectory of the falling seeds. There may also be a region with less airflow disturbance under the rotor. In this paper, the wind field is simulated to find the location of the optimal seed guide. This is done to reduce the airflow disturbance on the seed trajectory. The environment for the simulation is built and the simplified model for the flow field calculation is shown in Fig. 9.

The flow field computational domain is modelled as a cuboid, which represents the operational environment in which the UAV is located. The rotating region where the propeller is located represents the dynamic domain grid. The face ABCD of the rectangular body is set as the velocity inlet, the face EFGH is the pressure outlet, and the other faces are set as walls. The position of the airframe is 2.5 m from the bottom of the rectangular body and 1.0 m from the top, and the rotational speed of the propeller is set to 2000 r/min in the dynamic domain to simulate the three-dimensional CFD (Computational fluid dynamic) model of the downwash airflow of the UAV at the flight speeds of 1.9 m/s, 2.2 m/s, and 2.85 m/s, and the hovering state, respectively. The velocity maps of different planning surfaces are also analyzed to explore the distribution law of the airflow.

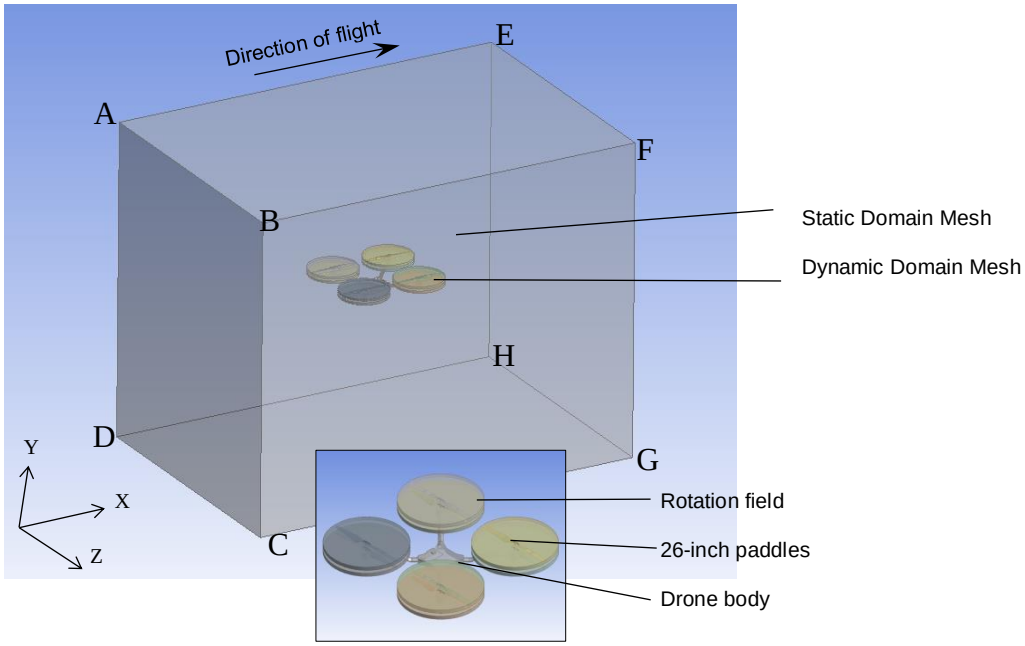

Boundary conditions:
Velocity inlet: ABCD surface
Pressure outlet: EFGH surface
Wall: other surfaces
Flow field material: air
Fuselage material: carbon braze, aluminium
Calculation model: k-epsilon (realizable)

Fig. 9 - Simulation environment construction

Method

Field seeding effect test

1. Seeding system bench test

Through the bench test, verify whether the various row seeding performance of the system meets the agronomic requirements of rice sowing.

1.1 Determination of test indexes

Referring to the test method stipulated in "NY/T3881-2021 Technical Specification for Quality Evaluation of Remote-Controlled Flying Seeder", the test indicators are the coefficient of variation of the discharge rate of each row (CVR) and total seed discharge rate stability (CVT) and breakage rate P, and the calculation formulas are as follows, respectively:

$$C_{vT} = \frac{\sqrt{\frac{1}{i-1}\Sigma(x_i - x)^2}}{x} \times 100\% \quad (1)$$

$$C_{v_R} = \frac{\sqrt{\frac{1}{j-1}\Sigma(y_j - y)^2}}{y} \times 100\% \quad (2)$$

$$P = \frac{m_i}{m_1} \quad (3)$$

x is the mean total discharge per unit of time, g/min; x_i is the total discharge per unit of time for the i-trial, g/min; y is the mean row discharge, g/min; y_i is the discharge for the jth row, g/min; CVR is the coefficient of variation of the discharge rate for each row, and CVT is the coefficient of variation of total seed discharge rate stability.

1.2 Test program and materials

The test scheme was to fix the UAV and the row seeding operation task platform on a 150mmx80mmx9mm table made of aluminum profiles as shown in Figure 10. In this paper, the pill box was used instead of the seed box to complete the test subsequent customized large-scale specifically for this shape of rice seed box. In this paper, the pill granulation of rice seeds was considered as a test object, and the sample bags were fixed at the mouth of the seed guide tube, to receive the rows in the amount of seed discharged per unit of time. Setting the groove wheel speed at 45 r/min (using the seventh channel of the remote control) corresponded to the degree of openness of 0%, 26%; setting the groove wheel speed at 30 r/min corresponded to a degree of openness of 58%, 71%. The weight of seeds discharged from each row was collected and recorded within 1 minute using a counting bag, from which the quality of broken seeds was screened to calculate the breakage rate. In the experiment, to facilitate the calculation of seed weight, the mass of the seed-coated fertilizer was not removed and the coated seeds were weighed directly.

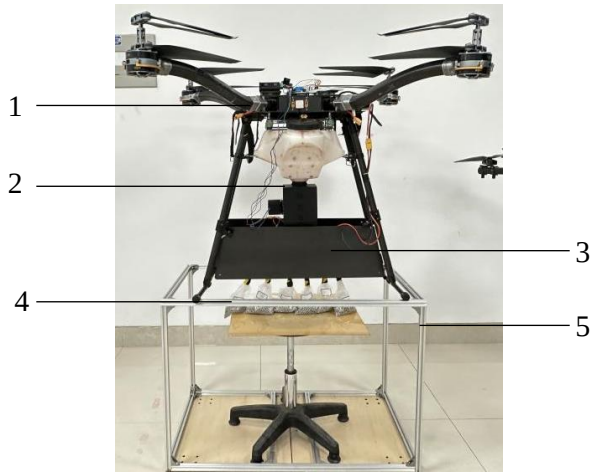

Fig. 10 - Bench test of seed discharge performance
1 - drone flying platform; 2 - grooved wheels; 3 - seeding device; 4 - counting bag; 5 - table stand

2. Sample machine field test trials

2.1 Test program and materials

The prescribed UAV flight height setting was based on the pre-simulation results derived from the seed guide tube mouth at a distance of 0.9 m from the rotor surface for the test; the flight altitude was set at 1.2 m, the flight speed at 1.5-2.5 m/s. The test site was in the Shandong University of Science and Technology, on the lawn behind the library, this place is wide open and unobstructed. On the day of the test the environmental winds were south-easterly winds, 1-3.5 m/s, the air humidity was 25%. Six rows of mud boxes (containing water, simulating a rice field) were arranged as shown n Figure 11, with a width of about 2.3 m, and the target sowing effect was 1.8 m, covering the maximum sowing width. The UAV flew over the mud box several times and recorded the probability of the number of seeds and the corresponding number of seeds at 250 positions continuously according to the national rice sowing enforcement standards. The pass rate, miss seeding rate and re-seeding rate were tested at different angles of the baffle. Records were repeated three times and averaged.

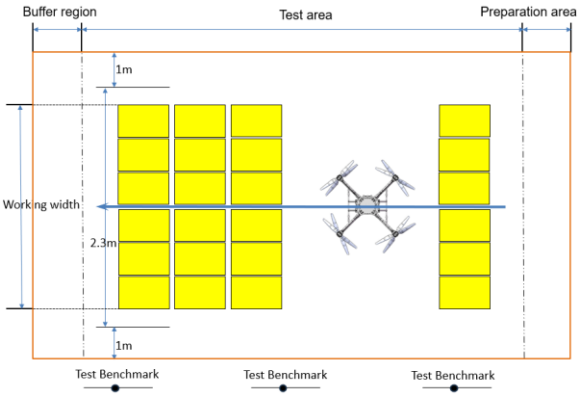

a. test plan view

b. test process view

Fig. 11 - UAV seeding performance test

2.2 Test indicators

There were four indicators of the test: pass rate, reseeding rate, leakage rate, breakage rate.

$$M_j = \frac{n_{m_j}}{N} \times 100\% \quad (4)$$

$$Q_j = \frac{n_{Q_j}}{N} \times 100\% \quad (5)$$

$$R_j = \frac{n_{R_j}}{N} \times 100\% \quad (6)$$

$$p = \frac{m}{M_n} \times 100\% \quad (7)$$

RESULTS

Determination of seed guide port position parameters

After several simulations, the velocity clouds of the UAV wind field at different speeds at different angles were derived as follows in Figure 12.

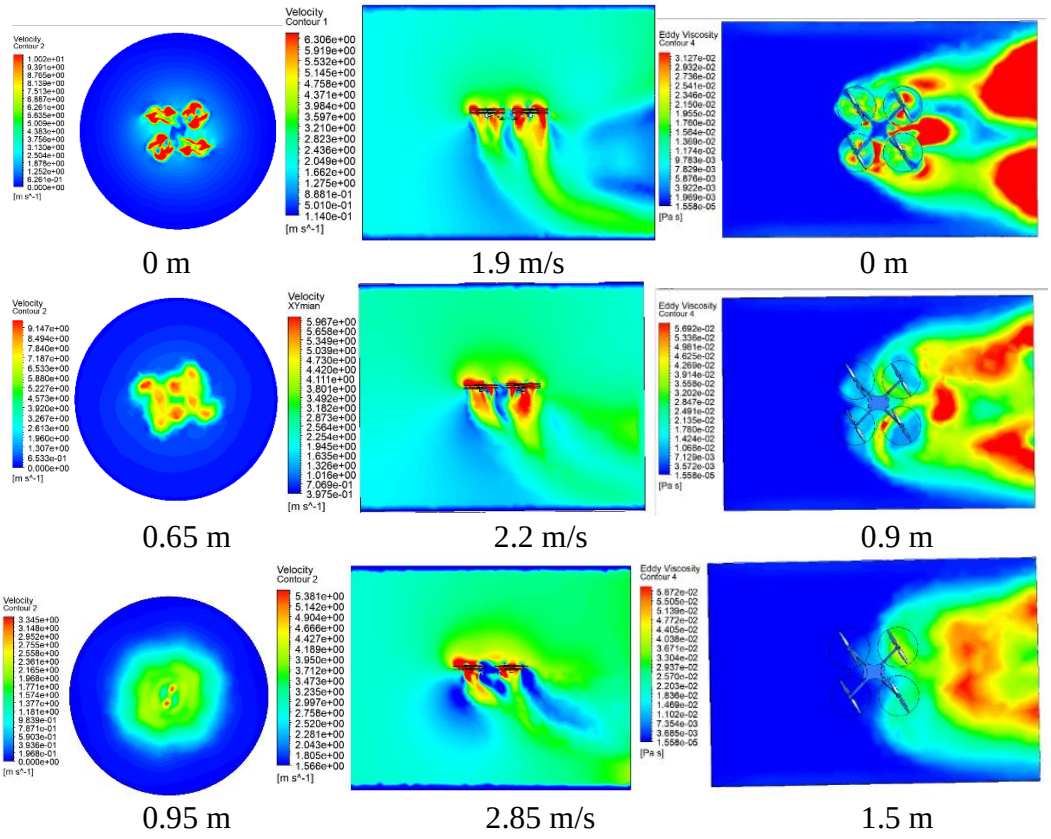

Fig. 12 - Velocity clouds at different angles of the flow field in which the UAV was located

The surface where the paddle was located was set as the horizontal plane. The velocity cloud of the XZ surface was observed at 0 m, -0.65 m, and -0.95 m from the horizontal plane respectively through the simulation post-processing software CFD-Post. From the first column of the three graphs in Fig. 12, it can be seen that the airflow was relatively concentrated at 0 m, and the airflow velocity was relatively high, and the airflow was distributed in four regions; at -0.65 m, the airflow in the corresponding regions of the four rotors gradually started to contract in one region but did not form a region completely, and its airflow velocity started to decrease; at -0.95 m, the airflow basically formed a region, and the airflow velocity was obviously reduced. At -0.95 m, the airflow basically formed a region, and its airflow speed decreased significantly.

From the second column of graphs, it can be seen that when flying at three different speeds, at 1.9 m/s, the airflow was shifted at -1.2 m; at 2.2 m/s the airflow was deflected at -1.0 m; at 2.85 m/s, the airflow was deflected at -0.85m. The velocity cloud maps from different heights during flight showed the distribution of the UAV in the XZ plane. The rotor flow field velocity distribution was symmetrically distributed with the centerline of the UAV fuselage, and along the -Y direction, the airflow was gradually weakened and shifted backward. When the UAV was flying at a speed of 2.85 m/s, the rotor airflow velocity around the fuselage was stronger at y=0 m; between y=0 m and y=-0.9 m, the airflow velocity was stronger, and mainly downward mixing was distributed; between y=-0.90 m and y=-1.5 m, the airflow velocity distribution showed a tendency to move backward and downward (with respect to the flight direction);

Taking flight safety as the premise, the fuselage should not fly close to the ground, and comparing the airflow fields at three different heights, it was found that the airflow velocity gradually decreased with the decrease of height when hovering, and the airflow velocity distribution showed a backward trend when flying forward, and the airflow velocity was the smallest directly under y=-0.9 m. Therefore, the seed guide orifice is arranged at a distance of 0.9 m below the paddle blade, which was conducive to reducing the influence of the rotor airflow velocity on seed drift after seed dropping.

Bench test data and result analysis

According to the 'NY/T3881-2021 Technical Specification for Quality Evaluation of Remote-Controlled Flying Seeders', CVR is less than or equal to 5 percent, CVT is less than or equal to 2.6 percent, and the rate of breakage is less than or equal to 2 percent. According to the regulations, the data from multiple trials of CVR can be used to represent the working level as the average of the data. As can be seen from the following table and figure, CVT, CVR, and breakage rate are low, and their maximum values are 0.84%, 1.88%, and 0.95% respectively, which all satisfy the indexes, and the seeding rate of each seed guide tube mouth has small ups and downs and is stable. When the rotational speed is 45 r/min, the seed guide tube seeding rate is the maximum of 2995 g/min, and as the volume of the groove increases the displacement of seeds is gradually increasing. Through the analysis of the device seed discharger design is in line with the requirements of practical applications.

Table 1

Bench test results of the fly-by-wire device

Flap opening	Row-by-row seeding / g						Total displacement /g·min^{-1}	CVR / %	CVT / %	Average value / %	Breakage rate / %
	1	2	3	4	5	6					
0%	2920	2941	2967	2986	2912	2901	17552	1.13			
	2906	2938	2995	2973	2934	2882	17531	1.41	0.17	1.32	0.22
	2913	2925	2976	2986	2918	2875	17593	1.42			
26%	1848	1887	1892	1889	1890	1856	11262	1.04			
	1850	1903	1903	1868	1860	1852	11236	1.29	0.11	1.17	0.29
	1841	1901	1886	1891	1874	1861	11254	1.16			
58%	754	753	778	785	761	756	4587	1.78			
	757	752	787	782	782	760	4620	1.98	0.42	1.88	0.63
	748	759	761	785	778	754	4585	1.87			
71%	401	413	417	419	411	403	2464	1.78			
	408	406	421	427	415	416	2493	1.89	0.84	1.80	0.95
	410	413	423	423	426	410	2505	1.74			

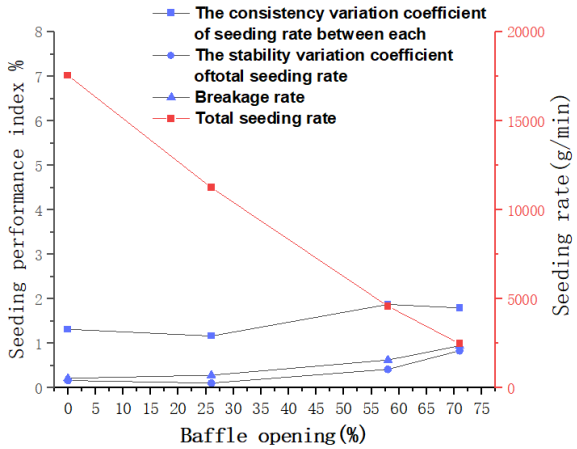

(a) Total seeding rate and coefficient of variation with respect to baffle opening

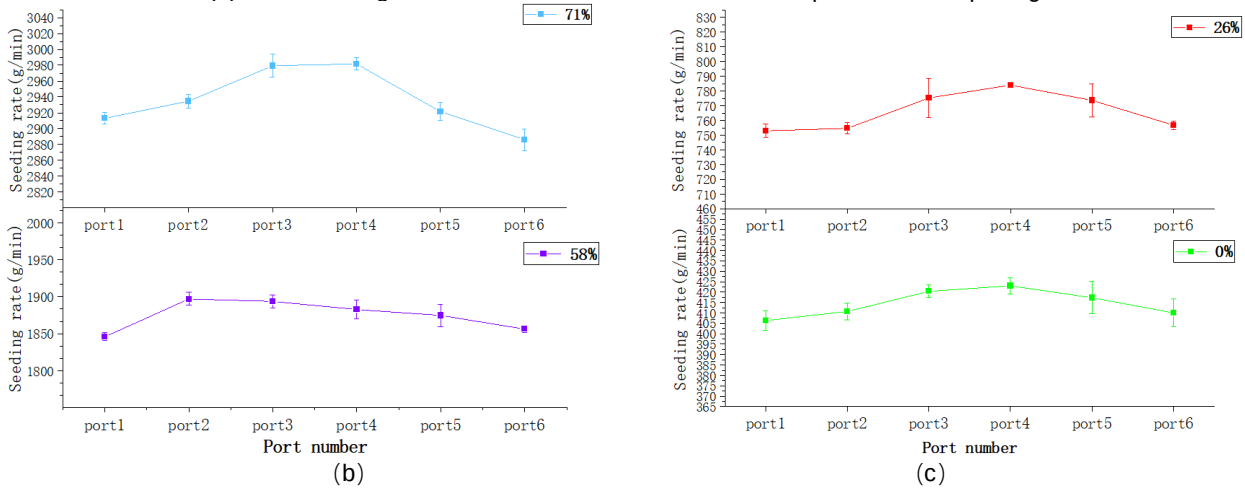

(b) (c)

(b) and (c) Comparison of seeding rates of each port

Fig. 13 - Seeding performance

The aircraft was fixed on the pedestal and the mud box was moved below to test the planting effect of the device as shown below:

Table 2

Effectiveness at different effective lengths

Flap opening	Number of particles	Satisfactory rate/%	Leakage rate/%	Rebroadcast rate/%	Breakage rate/%
71%	1-3	89.56	2.23	8.21	0.81
58%	3-5	90.64	2.11	6.25	0.55
26%	5-10	93.77	2.13	4.10	0.43

Site test data and data analysis

Through the change of the grooved wheel baffle to control the volume of different individual holes of the grooved wheel, the test analysis was carried out, and it was verified that the fly sowing device based on the UAV platform could achieve effective sowing for points with different numbers of seeds as shown in Figure 14 below. Due to the characteristics of the use, the rice seeds unlike fertilizers, pesticides, etc. cannot be used in excess. In order to ensure the overall pass rate, the volume of grooved wheel grooves was designed with redundancy. The purpose was to reduce the leakage of sowing, so it could be appropriate for more seeds. The trial was conducted at a minimized flight speed to satisfy a moderate or redundant amount of seed at each position. The aim was to reduce the probability of missed sowing and to guarantee that the yield of rice would not be reduced at a later stage. According to the experimental test under three different effective lengths of the grooved wheel, when the rotational speed of the grooved wheel was 45 r/min and the baffle opening was 26%, the qualification rate was 88.94%; when the rotational speed of the grooved wheel was 30 r/min, at the time of the baffle opening of 58%, the qualification rate was 86.89%, and at the time of the baffle opening of 71%, the qualification rate was 86.18%, and its sowing effect was very close to the ground effect of mechanical operation. However, when the position of the seed guide was higher, after 2 m and 2.5 m tests, the pass rate was 83.4% and 76.8%, the effect was not as good as for the height of 1.2 m. The reason may be that the trajectory of the seeds was affected by the wind force of the drone. The results weren't as good as the indoor tests because of the effects of the drone's wind.

1-3 Grain/placement 3-5 Grain/ placement 5-10 Grain/ placement Strip seeding

Fig. 14 - Schematic diagram of sowing effect

Table 3

Effectiveness at different effective lengths

Flap opening	Number of particles	satisfactory rate/%	leakage rate/%	reseeding rate/%	breakage rate/%
71%	1-3	86.18	3.16	10.66	0.73
58%	3-5	86.89	2.84	10.27	0.45
26%	5-10	88.94	2.47	8.59	0.31

CONCLUSIONS

(1) In order to solve the problem that the wind field disturbs the trajectory of falling seeds and causes the seeds to be unable to be arranged in equidistant rows when the UAV is spreading rice, a shot seeding device that can sow five rows of pelleted rice seeds at the same time was designed. The unit was centered on an external grooved wheel seed metering device and a seed acceleration unit for row seeding and hole sowing. The general control system and the process of seeding unit design are described.

(2) In order to reduce the influence of the airflow in the wind field of the UAV on the trajectory of the seeds, the characteristics of the airflow changes below the paddles during the operation of the UAV were analyzed. The variation of the cross-section velocity cloud map at different heights under a hovering state was analyzed and the result that the wind speed was smaller at 0.95 m was obtained. The change of velocity cloud map in XY plane under the flight speed of 1.9 m/s, 2.2 m/s and 2.85 m/s was analyzed and it was concluded that the wind field was shifted at 0.85 m when the drone is working at 2m/s.

Taking into account, that the minimum area of airflow disturbance was 0.9 m from the rotor surface, it was determined that the optimal position of the seed guide was 0.9 m from the rotor surface, in order to guarantee the accuracy of the seed drop point.

(3) The results of the indoor tests showed that the greater the angle of the baffle, the smaller the number of seeds in each position on the ground. When the baffle angle was 26%, 58%, and 71% respectively, the CVR was ≤1.88%, the CVT was ≤0.84%, and the breakage rate was ≤0.95%. The test results met the standards, indicating that the device met the operational requirements.

(4) The results of the outdoor mud box test showed that hole sowing and strip sowing could be realized when the sowing volume varied. The feasibility of this seeding method was verified. Compared with the traditional sowing operation, this device can ensure that the seed falling position is orderly, and can efficiently complete the hole sowing operation. The qualification rates of 1-3 seeds, 3-5 seeds, and 5-10 seeds were 86.18%, 86.89%, and 88.94%, respectively, and the test results were in line with the operational requirements.

ACKNOWLEDGEMENTS

This research was funded by the Ningxia Key Research and Development Plan Project (2023BCF01051); the National Key R&D Program of China, Large Load Plant Protection Intelligent UAV Creation and Application (2023YFD2000200). We would also like to thank the anonymous reviewers for their important suggestions and comments to improve our article.

REFERENCES

[1] Bian Z.H., Lan Y.B., et al. (2024). Effect of nozzle angle of plant protection unmanned aerial vehicle on droplet deposition distribution. *INMATEH - Agricultural Engineering*, Vol.72(1), pp. 214–223.

[2] Gao X.M., You Z.Y., Wu H.C., (2022). Design and testing of a green manure seed-spreading device based on a UAV platform [J]. *Transactions of the Chinese Society for Agricultural Machinery,* 53(11): 76-85.

[3] He W.Z., Liu W., Jiang R., et al. (2022). Control system design and experiments of UAV shot seeding device for rice [J]. Transactions of the CSAE, 38(18): 51-61.

[4] Huang X.M., Xu H.W., Zhang S., et al. (2020). Design and experiment of a rape aerial seeding in lines device[J]. *Transactions of the CSAE*, 36(5): 78-87.

[5] Huang X.M., Zhang S., Zhu Y.Z., et al. (2022). Seeding process analysis and test of the air conveying rapeseed aerial seeding device [J]. *Transactions of the CSAE,* 38(17): 31-41.

[6] Luo X.W., Xie F.P., Qu Y.G. et al. (2004). Comparative test of different planting methods for rice production [J]. *Transactions of the CSAE,* 20(1): 136 - 139.

[7] Luo X.W., Wang Z.M., Zeng S., et al. (2019). Recent advances in mechanized direct seeding technology for rice[J]. *Journal of South China Agricultural University*, 40(5): 1-13.

[8] Shen A., Zhou S.D., Wang M., et al. (2018). Simulation analysis of flow field of multi-rotor UAV[J]. *Flight Mechanics*, 36(4): 29-33.

[9] Song C.C., Zhou Z.Y., Zang Y., et al. (2020). Variable-rate control system for UAV-based granular fertilizer spreader[J]. *Computers and Electronics in Agriculture*, 180: 105832.

[10] Song C.C., Zhou Z.Y., Jiang R., et al. (2018). Design and parameter optimization of pneumatic rice sowing device for unmanned aerial vehicle[J]. *Transactions of CSAE*, 34(6): 80 − 88.

[11] Wan J.J., Qi L.J., Zhang H., et al. (2021) Research status and development trend of UAV broadcast sowing technology in China[C]//2021 ASABE Annual International Virtual Meeting. Michigan, USA: *American Society of Agricultural and Biological Engineers*, 1-12.

[12] Zeng S., Tan Y.P., Wang Y., et al. (2020). Structural design and parameter determination for fluted-roller fertilizer applicator. *International Journal of Agricultural and Biological Engineering,* 13(2): 101-110.

[13] Zhang H., Qi L.J., Wu Y.L., et al. (2019). Distribution characteristics of rotor downwash airflow field under spraying on orchard using unmanned aerial vehicle[J]. *Transactions of the CSAE*, 35(18): 44-54.

[14] Zhang, Q.S., Zhang, K., Liao Q.X., et al. (2020). Design and experiment of rapeseed aerial seeding device used for UAV. *Transactions of the CSAE*, 36, 138-147.

[15] Zhou Z.Y., Yuan W., Chen S.D., (2014). Current status and future directions of rice plant protection machinery in China[J]. *Guangdong Agricultural Sciences,* 41(15): 178-183.